Spatial distribution of radiation-induced defects in p^+-n InGaP solar cells

M. J. Romero,[a] D. Araújo, and R. García
Departamento de Ciencia de los Materiales e I.M. y Q.I., Facultad de Ciencias, Universidad de Cádiz, Apdo. 40, E-11510, Puerto Real (Cádiz), Spain

R. J. Walters and G. P. Summers
Naval Research Laboratory, Code 6615, 4555 Overlook Ave., S.W., Washington, DC 20375

S. R. Messenger
SFA, Inc., Largo, Maryland 20744

(Received 30 November 1998; accepted for publication 28 April 1999)

The spatial distribution of radiation-induced, radiative recombination centers in single-junction p^+-n InGaP solar cells irradiated by 1 MeV electrons or 3 MeV protons has been determined from cathodoluminescence (CL) spectra. The energy levels of the radiation-induced, nonradiative recombination centers were determined from the temperature dependence of the CL intensity. © *1999 American Institute of Physics.* [S0003-6951(99)05025-1]

The U.S. Naval Research Laboratory and the University of Cádiz, Spain, have established a collaborative research effort to study the radiation response of emerging space solar cell technologies. In this research, we combine the techniques of electron beam induced current (EBIC) and cathodoluminescence (CL) with more standard analysis techniques to allow a detailed characterization of the radiation-induced defects that control the solar cell radiation response. In addition to providing critical information on space solar cell technologies, this research also highlights the power and versatility of the EBIC and CL techniques for characterization of radiation-induced defects.

Specifically, in this letter, we have investigated the effects of 3 MeV proton and 1 MeV electron irradiation on single-junction (SJ) p^+-n $In_{0.5}Ga_{0.5}P$ (hereafter, InGaP) solar cells,[1] which are similar to the top cells of InGaP/GaAs/Ge dual-junction solar cells.[2,3] We have used CL produced by the electron beam in a scanning electron microscope (SEM) to determine the spatial distribution of the radiation-induced defects in the cells with submicrometric resolution. The energy levels of the defects that govern the emission efficiency are estimated from the temperature dependence of the CL intensity. Also, CL spectra taken from different regions of the cells at low temperature enable the spatial distribution of shallow energy level defects, acting as radiative-recombination centers, to be estimated.

The p^+-n SJ InGaP cells were grown by organometallic vapor phase epitaxy (OMVPE) on n^+ GaAs substrates at the Research Triangle Institute. Details of the solar cell heterostructure are described in Ref. 1. The CL experiments were carried out on a freshly cleaved {110} face perpendicular to the p^+-n InGaP junction. CL micrographs and spectra were excited using electron beam energies over the range 5–30 keV.

Since the range of 1 MeV electrons and 3 MeV protons (approximately 200 and 70 μm, respectively) is much greater than the depth of the p^+-n junction (approximately 0.5 μm), the particles traversed the InGaP region of the structure with relatively constant energy and finally stopped in the GaAs substrate. The CL investigation of the spatial distribution of the nonradiative recombination centers was therefore performed in the GaAs.

The intensities of the CL peaks corresponding to the band-to-band transitions in the InGaP and GaAs regions were measured as a function of temperature. These results are displayed as Arrhenius plots in Fig. 1. Considering first the GaAs emission efficiency (η) data, Fig. 1 clearly shows two separate intervals where an Arrhenius dependence was followed. This behavior corresponds to two thermally activated nonradiative recombination mechanisms, which can be analyzed using Eq. (1):

$$\eta = \left[1 + \kappa^{\alpha}\exp\left(-\frac{E^{\alpha}}{k_B T}\right) + \kappa^{\beta}\exp\left(-\frac{E^{\beta}}{k_B T}\right)\right]^{-1}, \quad (1)$$

where κ is the ratio of radiative to nonradiative recombination lifetimes for each nonradiative recombination mechanism (labeled α and β) at $T = 300$ K and E^{α} and E^{β} are their thermal activation energies. The solid lines in Fig. 1 repre-

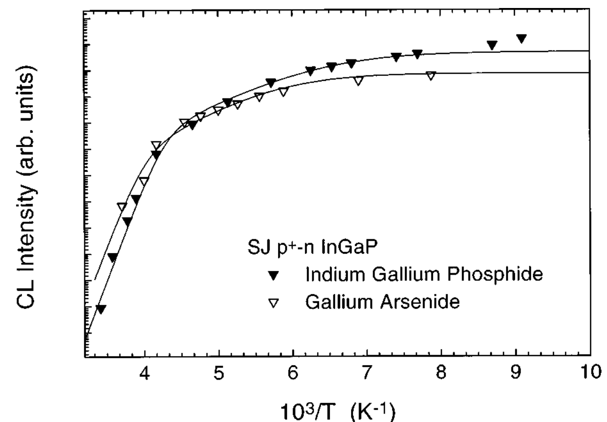

FIG. 1. Arrhenius plot of the temperature dependence of the InGaP and GaAs band-to-band luminescence intensity in the proton irradiated solar cells. The solid lines represent fits of the data to Eq. (1). The SEM electron beam energy was 20 keV at 1 nA.

[a]Electronic mail: manueljesus.romero@uca.es

 © 1999 American Institute of Physics
Downloaded 23 Mar 2006 to 150.214.231.66. Redistribution subject to AIP license or copyright, see http://apl.aip.org/apl/copyright.jsp

sent fits of the measured data to Eq. (1). The fitting parameters for the GaAs emission efficiency were $E^{\alpha}=0.14\,\mathrm{eV}$, $E^{\beta}=0.64\,\mathrm{eV}$, $\kappa^{\alpha}\sim 10^4$, and $\kappa^{\beta}\sim 10^{14}$. The α recombination center is assumed to be the previously reported[4] electron trap $E2$ that is found in both electron and proton irradiated GaAs samples.[5] It has been suggested that the $E2$ defect may be an As interstitial and an As vacancy complex $(\mathrm{As}_i-\mathrm{V}_{\mathrm{As}})$, next to electron traps $E3$ and $E5$.[6] The difference in the trap levels for $E2$, $E3$, and $E5$ is a result of the respective $\mathrm{As}_i-\mathrm{V}_{\mathrm{As}}$ distance.[7]

A candidate for the β recombination center is the proton irradiation-induced electron trap labeled $P3$.[6,8] Since the temperature dependencies for both the proton and the electron-irradiated InGaP cells are similar, we suggest that the β center is probably related to the $E5$[6] electron trap for the electron-irradiated case.

The InGaP data shown in Fig. 1 appear to show three intervals where separate Arrhenius dependencies occur, suggesting that three thermally activated nonradiative recombination mechanisms were present. The experiments did not reach low enough temperatures to characterize the shallowest defect level (i.e., data below 120 K). However, such a defect is not expected to play a significant role in the operation of the cell since it is those defects closer to midgap that are expected to control the solar cell performance. Therefore, the shallowest defect was ignored in the present analysis, and the measured data were fit to Eq. (1) assuming only two recombination mechanisms yielding values for the parameters of $E^{\alpha}=0.14\,\mathrm{eV}$, $E^{\beta}=1.25\,\mathrm{eV}$, $\kappa^{\alpha}\sim 10^4$, and $\kappa^{\beta}\sim 10^{15}$. Similar analysis of the CL data following electron irradiation also yielded a defect level near 1.25 eV. This is consistent with the results of Walters *et al.*[1] where the radiation-induced increase in junction dark current of InGaP solar cells (the same cells as measured here) was found to be due to a radiation-induced defect with an activation energy near 1.25 eV. This level is close to the $IE3$ level reported by Zaidim *et al.*[9] The large value of κ^{β} indicates that it is a highly efficient recombination center.

The CL signal was also measured at both 300 and 110 K (Fig. 2) as a function of depth into the cell. Because the epitaxial layers in the InGaP region were so thin, these measurements were made almost entirely in the GaAs substrate. At 300 K, the CL efficiency is controlled by the 0.64 eV defect level that has been tentatively associated with the defect labeled $P3$. Therefore, any spatial variation of the CL signal can be attributed to the spatial distribution of this nonradiative recombination center. At 110 K, on the other hand, the nonradiative recombination center with activation energy of 0.14 eV (which seems to be associated with the $E2$ defect) controlled the emission efficiency. At 110 K, therefore, the spatial distribution of the $E2$ center determined CL luminescence.

It can be assumed that the CL intensity as a function of depth into the cell follows the inverse of the distribution of nonradiative recombination centers: $E2$ at $T=110\,\mathrm{K}$ and $P3$ ($E5$ for the electron-irradiated case) at $T=300\,\mathrm{K}$. If this is the case, the distribution of the 0.64 eV defect appears to be uniform up to the particle range for both the electron and proton irradiations. However, the $E2$ defect distribution is different following electron and proton irradiations. After the electron irradiation, the distribution appears to be highly uniform with a slight increase close to the electron range (~200 μm), but after proton irradiation, the defect concentration appears to increase almost linearly with increasing depth throughout the full range of the protons.

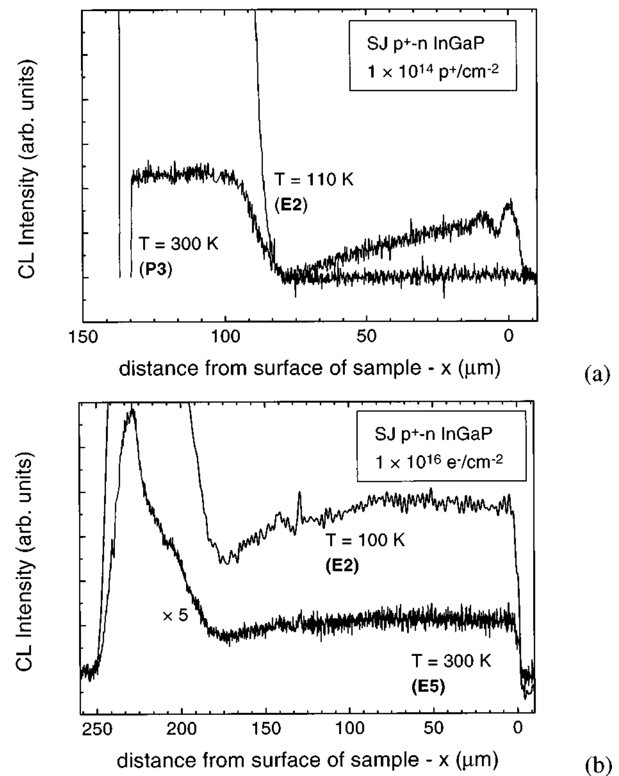

FIG. 2. CL intensity measured as a function of depth into the InGaP solar cells under proton (a) and electron (b) irradiation. Data were measured at 300 and 110 K. The spatial distribution of the CL intensity is assumed to be an inverted mapping of the nonradiative recombination center concentration. The maximum penetration depths of both 3 MeV protons and 1 MeV electrons are directly estimated from these CL data.

The difference in defect distributions observed following the electron and proton irradiations probably arose from differences in the rate of energy loss in the two cases. The rate at which defects are produced is usually proportional to the displacement damage energy transferred from the incident particle to the lattice, which in turn is proportional to the nonionizing energy loss (NIEL). The NIEL of 3 MeV protons in GaAs is about 2 orders of magnitude greater than that of 1 MeV electrons. Also the NIEL increases with decreasing proton energy while the opposite is true for electrons. Therefore, the protons slow down more rapidly as they penetrate the material (as evidenced by the much shorter range of the protons) and create more defects per linear distance into the sample than the electrons, and with a pronounced peak at the end of the range (the Bragg peak).

Interesting effects were observed in the CL data measured near the Bragg peak of the irradiating protons (i.e., ~70 μm). Figure 3 shows CL spectra measured at a depth just above and just below 50 μm. As the measurement depth approaches the proton range, two radiation-induced, broad luminescence bands are seen to emerge. These bands are peaked at energies of approximately 1.41 and 1.22 eV, and they are tentatively attributed to transitions involving As vacancy and silicon acceptor $(\mathrm{V}_{\mathrm{As}}-\mathrm{Si})$,[10] and donor silicon

Downloaded 23 Mar 2006 to 150.214.231.66. Redistribution subject to AIP license or copyright, see http://apl.aip.org/apl/copyright.jsp

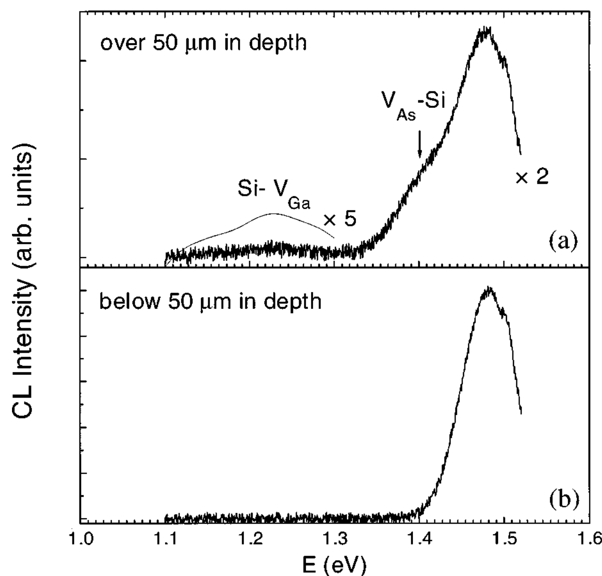

FIG. 3. The CL spectra measured at 70 K in the GaAs substrate. These spectra were measured at a depth just under (a) and just over (b) 50 μm. As the measurement depth increases, two CL peaks are seen to emerge that may be associated with Ga and As vacancy defect complexes. The line is a guide to the eyes for the 1.22 eV peak.

and Ga vacancy $(\mathrm{Si-V_{Ga}})$[11] defects, respectively. These shallow defects are detected through the CL measurements after the protons have lost a large fraction of their incident energy (i.e., near the proton range) where the protons are imparting a large amount of energy to the lattice. Figure 4 shows the intensity profile of the As vacancy related emission estimated from the CL spectra collected at different depths (the Ga vacancy related emission is difficult to estimate because the emission intensity is too low to detect). It is clear that As vacancies are generated up to the proton penetration depth with a maximum concentration near the projected proton range.

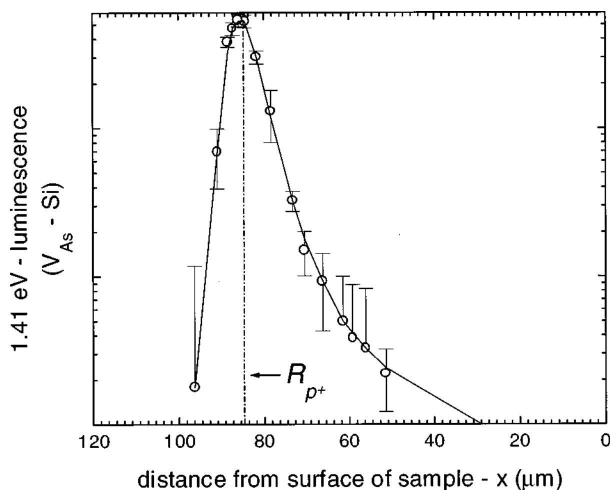

FIG. 4. The intensity profile of the As vacancy related emission estimated from the CL spectra collected at different depths near to the projected proton range in the proton irradiated samples. The defect concentration is seen to peak sharply near the end of the proton range.

In this letter, the usefulness and versatility of the CL technique for studying radiation-induced defects with high spatial resolution is demonstrated. In active layers of the InGaP solar cell, both the electron- and the proton-induced degradation is attributed mainly to a highly efficient recombination level at 1.25 eV, which is close to the $IE3$ defect level and which is consistent with the measured degradation of the photovoltaic parameters of InGaP solar cells. In the GaAs substrate, radiation-induced recombination centers located at 0.14 (associated with the defect labeled $E2$) and 0.64 eV (associated with the defects labeled $E5$ and $P3$ for the electron- and proton-irradiated cells, respectively) govern the emission efficiency. The electron irradiation introduces defects uniformly throughout the sample while the proton-induced defect concentration increases with depth into the solar cell. In the proton irradiated solar cells, detailed analysis of the CL data indicated a spike of Ga and As related defects about 40 μm wide and centered near the projected proton range.

This work was supported at Cádiz by the CICYT (Comisión Interministerial de Ciencia y Tecnología) under MAT94-0823-CO3-02 and by the Junta de Andalucía through group TEP-0120. The U.S. Office of Naval Research supported, in part, the work at NRL.

[1] R. J. Walters, M. A. Xapsos, H. L. Cotal, S. R. Messenger, G. P. Summers, P. R. Sharps, and M. L. Timmons, Solid-State Electron. **42**, 1747 (1998).
[2] K. A. Bertness, S. R. Kurtz, D. J. Friedman, A. E. Kibbler, C. Kramer, and J. M. Olson, Appl. Phys. Lett. **65**, 989 (1994).
[3] J. M. Olson and D. J. Friedman, Compd. Semicond. **2**, 27 (1996).
[4] Landolt-Börnstein, *Numerical Data and Functional Relationships in Science and Technology: New Series, III/22b, Impurities and Defects in Group IV Elements and III-V Compounds* (Springer, Berlin, 1989), p. 598.
[5] F. H. Eisen, K. Bachem, E. Klausman, K. Koehler, and R. Haddad, J. Appl. Phys. **72**, 5593 (1992).
[6] D. Pons and J. Bourgoin, Phys. Rev. Lett. **47**, 1293 (1981).
[7] D. Stievenard, X. Boddaert, J. C. Bourgoin, and H. J. von Bardeleben, Phys. Rev. B **41**, 5271 (1990).
[8] Y. Yuba, M. Matso, K. Gamo, and S. Namba, Proceedings of 13th International Conference on Defects in Semiconductors, Colorado, Aug. 1984 Metallurgical Soc. of AIME (unpublished), p. 273.
[9] M. A. Zaidim, M. Zazoui, and J. C. Bourgoin, J. Appl. Phys. **73**, 7229 (1993).
[10] E. V. K. Rao and N. Duhamel, J. Appl. Phys. **49**, 3458 (1978).
[11] M. Ilegems, *Properties of III-V Layers in Technology and Physics of Molecular Beam Epitaxy*, edited by E. H. C. Parker (Plenum, New York, 1985).

Downloaded 23 Mar 2006 to 150.214.231.66. Redistribution subject to AIP license or copyright, see http://apl.aip.org/apl/copyright.jsp